JCTC Journal of Chemical Theory and Computation

# A Coarse-Grained Molecular Dynamics Study of Carbon Nanoparticle Aggregation

Sergei Izvekov[†] and Angela Violi*

*Department of Mechanical Engineering, University of Michigan, Ann Arbor, Michigan 48109*

Received January 21, 2006

**Abstract:** A multiscale coarse-graining procedure is used to study carbonaceous nanoparticle assembly. The computational methodology is applied to an ensemble of 10 000 nanoparticles (or effectively 2 million total carbon atoms) to simulate the agglomeration of carbonaceous nanoparticles using coarse-grained atomistic-scale information. In particular, with the coarse-graining approach, we are able to assess the influence of nanoparticle morphology and temperature on the agglomeration process. The coarse-graining of the interparticle force field is accomplished applying a force-matching procedure to data obtained from trajectories and forces from all-atom molecular dynamics simulation. The coarse-grained molecular dynamics results show rich and varied clustering behaviors for different particle morphologies. They are shown to reproduce accurately the structural properties of the nanoparticles systems studied, while allowing for molecular dynamics simulations of much larger self-assembled nanoparticles systems.

## Introduction

In combustion environments, soot formation (particles with an average size of thousands of nanometers) is a fascinating multiscale problem of nanoparticle growth, both in length scale and in time scale. Figure 1 shows the chemical and physical processes for the formation of nanoparticle agglomerates starting from simple molecules, going through the formation of polycyclic aromatics and particle inception, and ending up with particle coagulation and agglomeration leading to primary particles (50 nm in diameter).[1] The processes involved in the formation of particles exhibit a wide range of time scales, spanning pico- or nanoseconds for intramolecular processes to milliseconds for intermolecular reactions. At the same time, the length scale also undergoes significant changes, going from a few angstroms for small polycyclic aromatic hydrocarbons to hundreds of nanometers for particle aggregates.

When the nanoparticles are able to reach a critical size (which is not always the case), they begin to aggregate on two separate length scales. The assembly on the smallest of these scales seems to be governed by the strongest interparticle interactions, so interesting patterns reminiscent of a spinodal decomposition process become evident. These smaller assemblies will, in turn, aggregate on an even larger

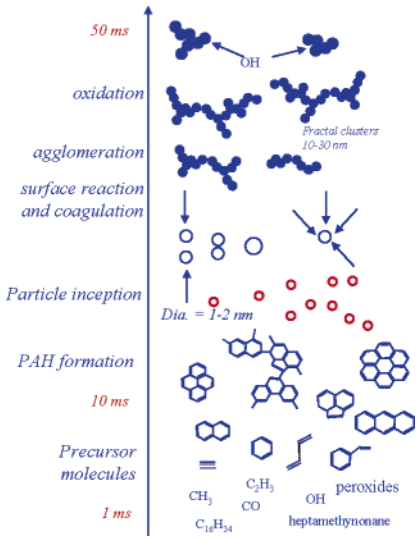


***Figure 1.*** Particle formation in flames.

* Corresponding author phone: (734) 615-6448; fax: (734) 647-9379; e-mail: avioli@umich.edu.

[†] Permanent address: Department of Chemistry, University of Utah, Salt Lake City, UT 84112.

10.1021/ct060030d CCC: $33.50 
Published on Web 04/26/2006

length scale through a process that resembles colloidal nucleation. Thus, the molecular science of the nanoparticles bridges with the statistical mechanics of nonequilibrium self-assembly and nucleation over two disparate length and time scales in a truly fascinating way.

These nanoparticles are quite robust and, in fact, stabilize a remarkably large number of radical sites on their surfaces. The high concentration of radical sites, along with the small size of the nanoparticles, leads to serious health implications when a person breathes these particles into their lungs.

This paper reports on a new multiscale coarse-graining simulation approach for bridging the time and length scales in the growth of the carbon nanocluster self-assembly. After a description of the methodology, results are shown for the assembly of carbonaceous nanoparticles of different morphologies in the temperature range 1100−1600 K.

## Computational Methodology

Carbonaceous nanoparticle agglomeration is influenced by large length- and time-scale motions that extend to mesoscopic scales, that is, one micrometer or more in length and one microsecond or more in time. To increase the time and length scales accessible in simulations and to be able to simulate nanoparticle assembly, it is necessary to describe the particles on a more coarse-grained (CG) level. The strategy of these CG approaches is generally the same: to achieve a simpler description of the effective interactions in a given system while not losing the ability of the resulting models to predict the properties of interest. The existing approaches for obtaining effective CG potentials target the reproduction of a few average structural properties seen in atomistic simulations or experiments, for example, using an iterative adjustment of potential parameters starting from an approximation based on potentials of mean force,[2,3] or the Inverse Monte Carlo technique,[4] or they may be parametrized to match thermodynamic properties.[3−8] These approaches rapidly become computationally expensive and less reliable for systems with an "aggressive" coarse-graining, such as the nanoparticles systems. Recently, a novel approach for a reconstruction of CG potentials from an underlying explicit atomistic molecular dynamics (MD) simulation has been proposed.[9−11] The method, which is called "multiscale coarse-graining" (MS−CG), is built upon the force-matching (FM) technique developed in ref 9. The MS−CG method exploits the fact that an application of the FM procedure to the CG images from underlying atomistic trajectory/force data should produce the effective interaction between CG structural units as it seen in the atomistic dynamics. The most obvious way to map an atomic group into a CG site is to associate it with its center of mass (CM) because the force acting on the CM of the atomic group can be straightforwardly evaluated from the atomistic MD data.

The algorithmic development of the MS−CG method is presented elsewhere.[9,12−14] In the MS−CG framework, the site−site force $\mathbf{f}_i^p(r_{ij}) = f^p(r_{ij})\mathbf{n_{ij}}$ (acting from site $j$ on site $i$), where $r_{ij}$ is the modulus of the vector $\mathbf{r}_{ij} = \mathbf{r}_j - \mathbf{r}_i$ connecting two sites and $\mathbf{n}_{ij} = \mathbf{r}_{ij}/\mathbf{r}_{ij}$, was represented by the cubic splines connecting a set of points $\{r_k\}$ with $r_{k\max}$ equal to the cutoff, was used to represent the $f(r)$

$$f(r,\{r_k\},\{f_k\},\{f''_k\}) = A(r,\{r_k\})f_i + B(r,\{r_k\})f_{i+1} + C(r,\{r_k\})f''_i + D(r,\{r_k\})f''_{i+1} \quad (1)$$

with $r \in [r_i, r_{i+1}]$.

In eq 1, $A$, $B$, $C$, and $D$ are known functions of $r$ and $\{r_k\}$, and $\{f_k\}$ and $\{f''_k\}$ are tabulations of $f(r)$ and its second derivative on a radial mesh $\{r_k\}$. The parameters $\{f_k, f''_k\}$ are to be obtained from the fit. The choice of spline is advantageous for two reasons. First, it preserves the continuity of $f_i^p(r_{ij})$ and its first two derivatives and gives the flexibility of fitting arbitrary pairwise forces. Second, a spline is a linear form of its parameters $\{f_k, f''_k\}$ and therefore permits a reduction of the least-squares problem in the force-matching procedure[15] to an overdetermined system of linear equations.[11,16]

A linear dependence of the force on the fitting parameters permits a splitting of the least-squares fit into two phases, making the whole procedure computationally much less expensive. Practically, the MS−CG method is implemented as follows. All sets of atomic configurations recorded along the trajectories of the reference MD simulation are partitioned into blocks, each containing $L$ configurations. For each block, the reference total force $\mathbf{F}^{\mathrm{ref}}_{\alpha il}$ which acts on the $i$th atom of kind $\alpha$ in the $l$th atomic configuration of the block and the same force predicted using the representation in eq 1 are required to be equal

$$-\sum_{\beta=1,K}\sum_{j=1,N_\beta}[f(r_{\alpha il,\beta jl},\{r_{\alpha\beta,k}\},\{f_{\alpha\beta,k}\},\{f''_{\alpha\beta,k}\})]\mathbf{n}_{\alpha il,\beta jl} = \mathbf{F}^{\mathrm{ref}}_{\alpha il}$$
$$\alpha = 1, ..., \mathrm{K};\ i = 1, ..., N_\alpha;\ l = 1, ..., L \quad (2)$$

with respect to $\{f_{\alpha\beta,k}, f''_{\alpha\beta,k}\}$ which are force parameters. In eq 2, $r_{\alpha il,\beta jl}$ is the distance between atoms $\{\alpha i\}$ and $\{\beta i\}$ in the $l$th atomic configuration of the block; $N_\beta$ and $K$ are, respectively, the number of atoms of kind $\beta$ and the total number of atomic kinds in the systems, and $\{r_{\alpha\beta,k}\}$ is a spline mesh which might be for different $\{\alpha\beta\}$. The size $L$ of each block should be large enough to ensure that eq 2 overdetermines the force parameters. Standard equations which are linear with respect to $\{f_{\alpha\beta,k}, f''_{\alpha\beta,k}\}$ must be included into eq 2 for the $f(r)$'s first derivative, $f'(r)$, to be continuous across the boundary between two intervals.[17]

The solutions of eq 2 need to be averaged over all of the blocks to get the effective force field. More discussion of the MS−CG methodology is given in ref 9.

As a result of this new approach, the effective phase space of the system is significantly reduced in size, as is the number of costly force calculations. In the MS−CG approach, the CG parameters are therefore developed "on the fly" from the actual atomistic-level forces coming from a full MD "presimulation". Hence, the term "multiscale" is used for the MS−CG method, meaning that changes at the atomistic level of the force field will systematically propagate upward via the force-matching algorithm to the CG representation of the system. The MS−CG model will allow the simulations of the nanoparticle systems in this project to bridge upward in both length and time scale, so as to better access the properties influenced by those scales.

The capability of the MS−CG approach to develop the CG parameters "on the fly" from the actual atomistic-level forces coming from a full MD is very important in the study of particle formation in combustion. The newly nucleated particles grow by coagulation and coalescent collisions as well as surface growth. All these processes happen at the same time, and while the CG approach can describe particle coagulation, *the surface growth* needs to be carried out at the atomistic level. The changes that can occur on single nanoparticles because of surface growth at the level of the atomistic MD will propagate upward to the MS−CG effective force field via the force-matching algorithm in a multiscale fashion.

The MS−CG method has been successfully applied to several complex condensed-phase and biological systems.[9] The method proved to be workable for systems of carbonaceous nanoparticles.[18] This is an important result because the coarse-graining of nanoparticle systems presents a special challenge because of their shapes, that is, ranging from the highly symmetric C60 to more amorphous and irregular shapes. They also generally interact through the sum of many weaker interactions rather than via strong electrostatics in, for example, an aqueous environment.

The MS−CG method is computationally efficient, and this is an important feature of the approach because the coarse-graining of the system interactions may greatly reduce the transferability of the resulting models between different thermodynamic conditions. MS−CG allows fast parametrization of the CG force fields at the thermodynamic conditions of interest instead of using "universal" models that increase the reliability of the CG simulations.

## Results

**Molecular Models.** The initial configurations of the carbonaceous nanoparticles chosen for this study are obtained using a combination of kinetic Monte Carlo and MD methodologies (**A**tomistic **M**odel for **P**article **I**nception, or AMPI code). The AMPI code has been developed to study the transformations that occur during the transition from the gas phase to particle inception,[19−21] providing information on both the chemical structure and the configuration of the nanoparticles. The capability of the AMPI code has been validated in different conditions, and nanoparticles have been characterized in terms of chemical structure and components, and relationships between the structure and pathways, structure and properties, and structure and reactivity population of active sites have been addressed. In particular, computed properties of nanoparticles have been compared with experimental data in terms of H/C trends, particle morphology, depolarization ratio, and free radical concentration.

Figure 2a,b shows two representative structures obtained with the AMPI code in different combustion environments. These results, in turn, correlate with the curvature of carbon layers seen in high-resolution transmission electron microscopy images of combustion-generated nanoparticles produced in flames, which show a different curvature of the carbon nanoparticles containing an amorphous, graphitic, or fullerenic nanostructure.[22−24]

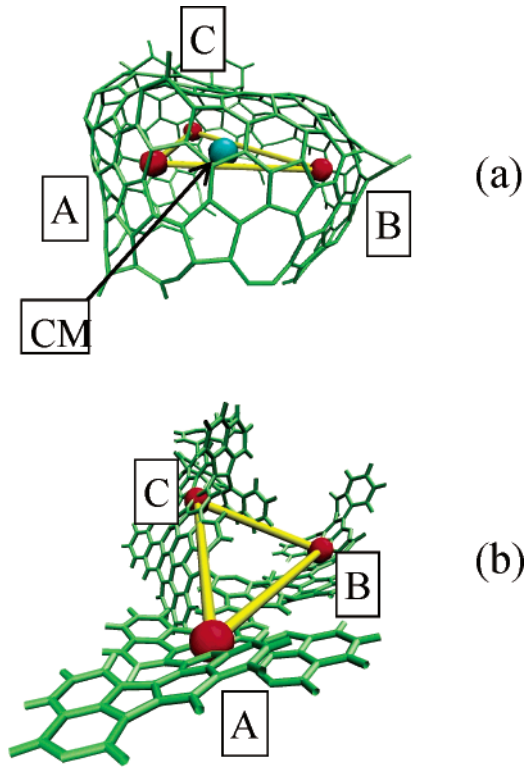


***Figure 2.*** Atomistic and coarse-grained representations of two carbonaceous nanoparticles: (a) round (one-site and three-site representations) and (b) flat (three-site representation).

The particle in panel (a), named "round", has an aspect ratio close to unity with a formula of $C_{188}H_{53}$, while the compound in panel (b) (the "flat" particle) has a composition of $C_{202}H_{90}$. Both round and flat nanoparticles have a size of around 17 Å in the longest dimension. The round precursor consists of a network of 5−8-membered fused rings such as buckyballs, whereas the flat one has four planar aromatic moieties connected by freely rotating bonds.

**CG Procedure.** To construct and validate an effective force field for CG unit interactions (force-matching algorithm), the following steps are required:

(1) Atomistic MD simulations of the particle ensembles

(2) Partitioning of the systems in CG sites and a buildup of the CG interactions

(3) Comparison between the CG results and the fully atomistic data

*1. Atomistic MD Simulation of the Particle Ensembles.* To address the importance of particle morphology on the assembly behavior, three ensembles are considered in this study: (1) 32 round nanoparticles, (2) 32 flat nanoparticles, and (3) 16 round and 16 flat nanoparticles.

The CHARMM force-field parameters[25] are utilized to describe the interactions between nanoparticles in a constant NVT ensemble. Figure 3 reports the snapshots from MD simulations at 1100 K for the three ensembles. It is important to note that the radical chemistry is not included in these simulations, and all dangling bonds of the carbon atoms on the nanoparticles have been hydrogen-terminated.

The round particles tend to cluster, and they show a preferred orientation that is back-to-back (left panel). Some

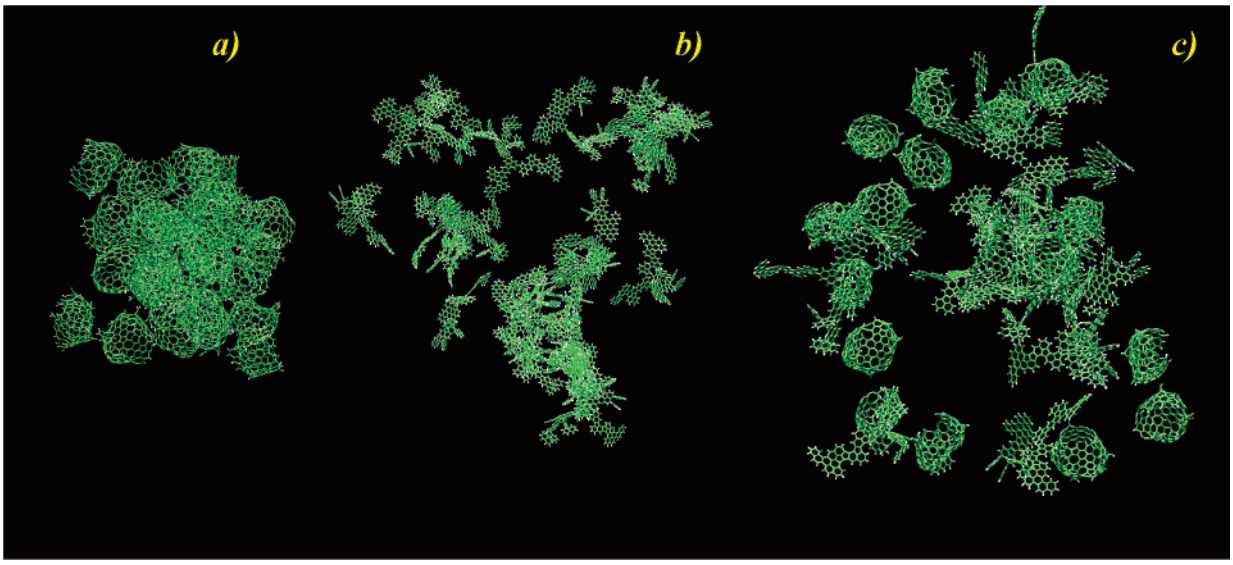


***Figure 3.*** Snapshots from MD simulations of three ensembles of 32 nanoparticles (panel a, "round"; panel b, "flat"; and panel c, "round/flat") at 1100 K.

of the sheetlike particles do cluster in small agglomerates (middle panel), while the third panel shows a snapshot of the mixed systems in which some of the particles drift away from the ensemble and some form subclusters. In addition, the clustering behavior for flat−flat particles is quite different from that for the round−round ones: the orientation is more edge-to-edge or stacking, and the interacting particles are tightly constrained.

The current models present in the literature report a simplified notion of the coagulation process, in which two particles coagulate after collision if the kinetic energy of the particles is lower than their interaction potential, which depends on van der Waals attraction and Born repulsion forces.[26] The results presented in Figure 3 show a much more complex process in which particle morphologies play an important role. This information is necessary to build a realistic model for particle formation.

*2. Partitioning of the System.* Carbonaceous nanoparticles can be coarse-grained into a different number of sites. Generally, a larger number of interaction sites is advantageous because the CG simulation yields a better resolution. However, a higher computational cost and a lower accuracy of the MS−CG procedure as well as a more expensive CG simulation are major drawbacks of such models.

As reported in ref 18, the one- and three-site models of the particles perform very well in reproducing the structural properties of the carbonaceous nanoparticles obtained in an all-atom MD simulation. Figure 2 shows the CG sites for the two nanoparticles studied here. The three-site model accounts for orientational degrees of freedom of the particles themselves, which are very important when dealing with complex processes, such as self-assembly or structural transitions of nanoparticles. For the first two ensembles (32 particles of the same morphology), a three-site CG representation is used. The "round" particles were mapped into a three-site geometry by slicing each of them into three segments of approximately equal weight by planes perpendicular to the opening plane of the particle. The CG interaction sites are associated with the CM of the corresponding segments as shown in Figure 2 (sites A, B, and C). Similar to the round particle, the flat nanoparticle is divided into three segments in accordance with its three "wings". The CG sites were associated with the CM of the corresponding segments as shown in Figure 2 (sites A, B, and C).

For the third system composed of 32 mixed particles, the one-site model is used for the round particles, in which the CG site is associated with the CM of the whole particle, and the three-site model for the flat particles. This choice allows the reduction of the computational time without losing accuracy.[18] In particular, for the 32-particle system, the acceleration of the simulation is about 2000−5000 times.

*2.1. Buildup of the CG Site Interactions.* MS−CG models with such an "aggressive" coarse-graining as those of one and three sites are expected to have a low transferability among different phases (e.g., at different temperatures and different densities). As an example, a MS−CG model generated from the all-atom simulation at a temperature of 1600 K to study particle aggregation at a lower temperature could be questionable. Ideally, the CG model has to be parametrized at the same thermodynamic conditions as those at which a simulation of the phenomena of interest is intended.

To assess the issue of transferability, MS−CG force fields for ensembles 1 and 2 of round and flat particles are computed at two temperatures (1100 and 1600 K) and two particle densities. The sizes of the supercells used for the simulations are 10.5 nm ("high" density) and 12.0 nm ("low" density), respectively. For the mixed system—ensemble 3—the MS−CG force field is calculated at 1600 K and for a single density (size of the supercell of 10.0 nm).

Data from the all-atom simulations are collapsed into trajectories and forces of the CG sites, and the resulting CG trajectory and force data are used as input to the FM algorithm. The trajectory and the force data from the atomistic simulations are sampled at an interval of 0.1 ps.

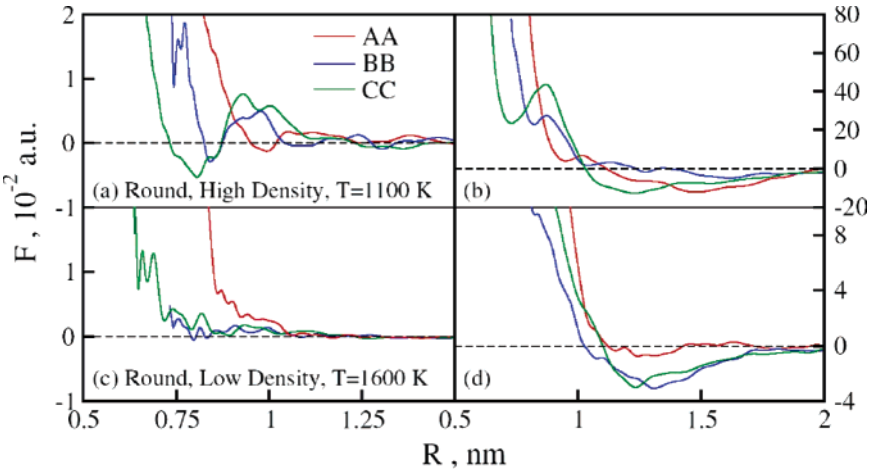


***Figure 4.*** Effective pairwise forces (left) and potentials (right) for selected pairs of CG sites as a function of the intersite separation calculated by the force-matching method. Panels a and b: round particles at 1100 K, "high" density. Panels c and d: round particles at 1600 K, "low" density.

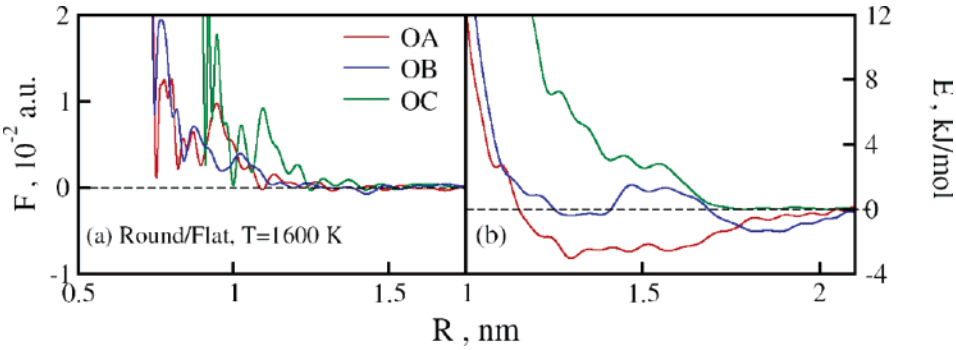


***Figure 5.*** Effective pairwise forces (left) and potentials (right) for the MS−CG model of the mixed system of round (one-site representation − O) and flat (three-site representation − A, B, and C) nanoparticles.

For the simulation at 1600 K and low density, the overdetermined system of linear FM equations is solved repeatedly for 15 000 sets of atomic configurations from 3.0 ns MD trajectory data, with each set consisting of two configurations ($L = 2$ in eq 2) and then averaged over all of the sets. For the other cases, the all-atom simulation is increased to 6.0 ns with a proportional increase in the number of sampled all-atom configurations.

The force field is represented by a spline over a mesh with a grid spacing of approximately 0.01 nm. The potentials are calculated by integrating out the respective terms in the force fields and then shifting them to zero at the cutoff radius. The classical MD simulations with the new CG models were performed using the DL_POLY 2.9 computer code.[27]

The tabulated force fields and potentials for the systems investigated in this paper are available in a DL POLY code format.

Figure 4 reports the diagonal effective potential profiles for the system of round particles at two temperatures and different densities. The effective forces appear to be less sensitive to a change in the average particle density than to variations in the temperature. As a consequence, the difference between the two force fields can be attributed mainly to a change in the temperature.

At 1600 K (Figure 4c,d), the strongest interactions are between the A−A and C−C pairs of sites, and the potential shows a minimum at −3.1 kJ/mol that is smaller than $k_BT$ = 13.3 kJ/mol at that temperature. At 1100 K, the binding energies of the A−A and C−C pairs dramatically increase to about −13 kJ/mol ($k_BT$ at 1100 K = 9.1 kJ/mol), with the equilibrium distances shifted toward long separation distances suggesting a possibility of aggregation. The similarity of potential profiles for different pairs of sites is just a manifestation of the high symmetry of the round particles.

An analogous tendency is observed for the system of flat particles. However, the binding energies are smaller at both temperatures (1100 and 1600 K) than those of the system of round particles and at the same time are below the values of

***Table 1.*** Properties of the Gas-Phase Dimer from Atomistic and CG Models of the Nanoparticles Parameterized at $T = 1600$ K and Low Density[a]

| model | $R_0$ (nm) | Upot (kJ/mol) | $\theta$ (deg) |
|---|---|---|---|
| round atomistic | 1.34 | −105.4 | 50.3 |
| round one-site | 1.23 | 7.5 | |
| round three-site | 1.35 | −16.74 | 44.5 |
| flat atomistic | 0.92 | −156.4 | 21.1 |
| flat three-site | 0.97 | 28.2 | 23.7 |

[a] Shown are $R_0$, the distance between centers of mass of particles; Upot, the interaction energy; and $\theta$, the angle between the planes through CG sites (for three-site models).

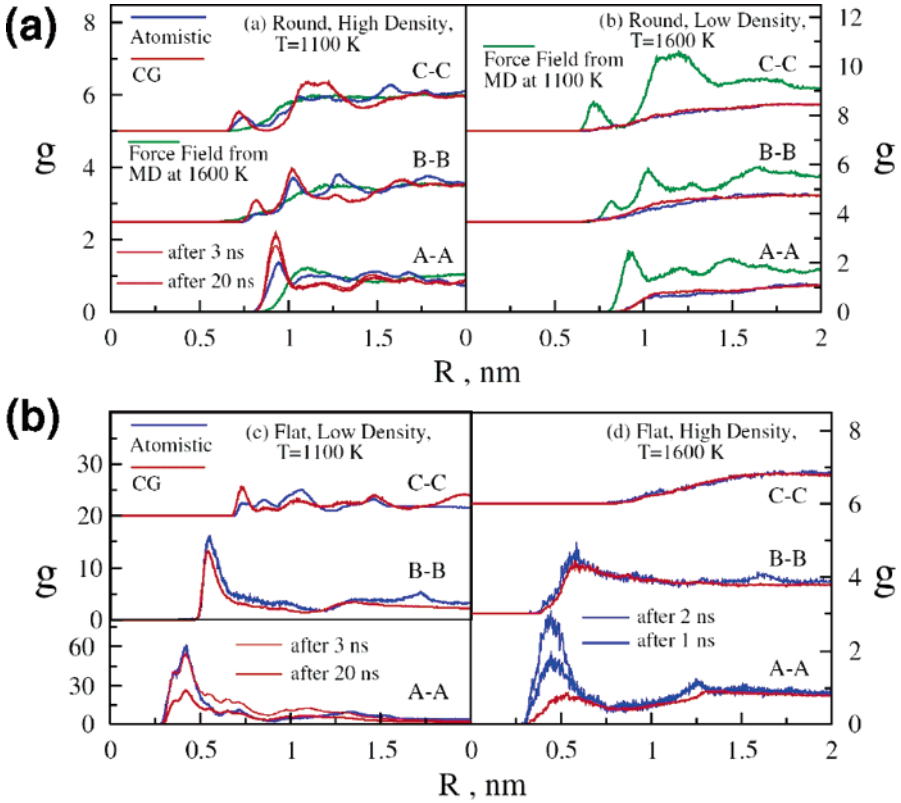


***Figure 6.*** (a) Comparison between selected RDFs of the all-atom MD simulations (blue lines) and those obtained from the MS−CG MD simulation (red lines) for ensemble 1—round particles—at 1100 and 1600 K. The green line represents the RDFs obtained using the force field computed at 1600 K (left panel) and 1100 K (right panel). (b) Comparison between selected RDFs of the all-atom MD simulations (blue lines) and those obtained from the MS−CG MD simulation (red lines) for ensemble 2—flat particles—at 1100 and 1600 K.

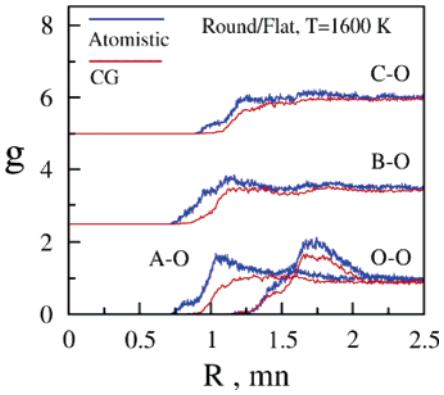


***Figure 7.*** Comparison between RDFs of the all-atom MD simulations (blue lines) and those obtained from the MS−CG MD simulation (red lines) for ensemble 3—round and flat particles.

$k_BT$. These results indicate some difficulties for the MS−CG flat particle ensemble to aggregate even at low temperatures.

For the mixed system—ensemble 3—Figure 5 shows the effective interactions of one-site round particles with three-site flat particles at 1600 K. The round particle tends to bind strongly to the A site of the flat particle, and the binding energy is comparable to the one obtained for the system of round particles—ensemble 1 (see Figure 4)—suggesting a stronger ability of the mixed system to aggregate compared with the system of flat particles—ensemble 2.

Because the all-atom simulation of the mixed system yielded poor statistics for the MS−CG procedure because of the small number of sites contained in the reference system compared with the system of flat particles, for the simulations reported below, we replace the interactions between flat particles with those from ensemble 2 obtained at 1600 K and low density.

*3. Validation of the MS−CG Models.* To test the MS−CG model, we first examine the properties of nanoparticle dimers in a vacuum. The results for the MS−CG model parametrized at 1600 K and low density are summarized in Table 1. The computed CG geometry of the dimers matches very well the data obtained from the atomistic model.

For the many-particle systems (ensembles 1−3), the MS−CG simulations are carried out using the same geometries and thermodynamic conditions as those of the reference all-atom system.

To check the transferability of the MS−CG models between different thermodynamic conditions, the structural properties obtained through the MS−CG model at different temperatures were compared with the results obtained at the all-atom level. The MS−CG simulations were initiated using the configuration which was final in the reference all-atom MD simulations. In Figure 6, some comparisons for the systems of interest are presented.

The MS−CG models perform very well in reproducing the reference structural properties: some discrepancies observed for the 1100 K simulations and for the high density

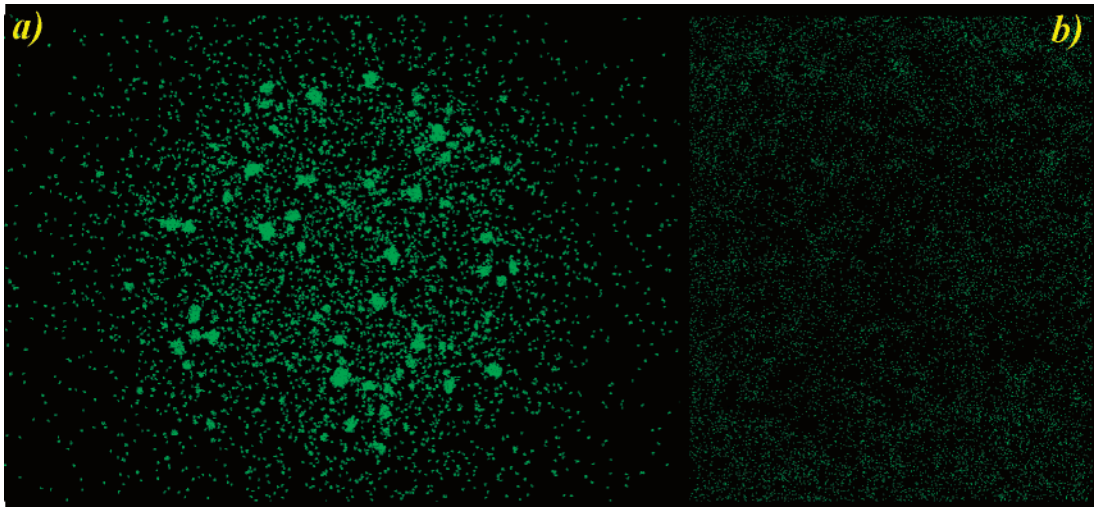


***Figure 8.*** Snapshots from CG MD simulations for 10 000 round (panel a) and 10 000 flat (panel b) nanoparticles at 1100 K. The CG modes were fitted to all-atom MD simulations at the same temperature.

simulations at 1600 K are due to the limited simulation time that caused the radial distribution functions (RDFs) in the all-atom simulations not to be fully converged. This conjecture is supported by a comparison of RDFs from the MS−CG simulations at early stages of the dynamics. Figure 6a, panel a, reports the RDF from the MS−CG simulation of the system of round particles at 1100 K: a first peak at the AA RDF recorded after 3 ns shows a better agreement with the atomistic value than the peak recorded after 20 ps. This suggests that the all-atom RDFs were indeed not fully converged.

It should be noted that, because the dynamics in the MS−CG MD simulation are significantly accelerated, a fair comparison of time scales between the MS−CG and all-atom simulations is difficult. Similar conclusions can be drawn looking at the RDFs from different simulations of the system of flat particles shown in Figure 6b, panels c and d.

In Figure 6a—panel (a)—the RDFs computed using the force field generated at 1600 K are shown as green lines, and the structure is dramatically different from that of the MS−CG model generated at 1100 K. The RDFs from the 1600 K model bear a memory of the structure at that temperature which is very different form the low-temperature case.

A similar comparison is reported in Figure 6a—panel (b)—when the MS−CG model parametrized at 1100 K is used to compute the RDF at 1600 K.

The failure of the MS−CG models to correctly reproduce the structure at temperatures different from those at which they were parametrized unequivocally points toward a very poor transferability of the MS−CG models of the nanoparticles.

The RDFs from the 1100 K simulations as well as those from the simulation at 1600 K and high density exhibit a significant number of peaks, which indicates the formation of particle agglomerates. The peaks tend to amplify as the simulations proceed, thus, further supporting the aggregation behavior in these systems.

Figure 7 shows the RDFs from the MS−CG simulation of the mixed system. Some mismatch between atomistic and MS−CG RDFs is, partly, due to the use of the MS−CG model derived from the flat particle simulation, to describe interactions of flat particles with each other. Relatively well pronounced peaks in the AO and OO RDFs indicate a significant tendency to aggregate for these pairs of sites.

**Behavior on Large Scales.** To study the formation of bigger agglomerates (soot primary particles), the MS−CG MD simulations are then conducted on a system of 10 000 CG particles (or effectively 2 million atoms) for 500 ns. The density chosen for these runs is $5 \times 10^{15}$ particles/cm$^{-3}$. Experimental data report a number concentration of around $1 \times 10^{14}$ for slightly sooting flames of ethylene.[28] However, the measured value is an average, and there are pockets inside the region of interest with higher density. The simulations reported in this paper are relative to those areas because higher density will increase the collision frequency and reduce the computational time required to form the first nuclei. Three ensembles are considered: (1) 10 000 round particles; (2) 10 000 flat particles, and (3) 5000 flat and 5000 round particles.

Figure 8 shows snapshots from the end points of the simulations for ensembles 1 and 2. The system of round nanoparticles clearly exhibits the presence of clusters at 1100 K, which are observed to persist for the entire length of the simulation. The cluster size was identified to be around 15−20 nm. The system of flat particles shows a much lower degree of clustering for the same temperature and density. These results confirm what had been observed in a more limited fashion at the microscale level and described earlier.

A fusion of two clusters of round particles as well as a split of the cluster into several fragments (typically two) has been frequently observed during the simulations, as well as an absorption of the "gas-phase" particles and an evaporation of nanoparticles from clusters.

A snapshot from the simulation of ensemble 3 of round and flat particles at 1600 K is shown in Figure 9. This system shows a better ability to aggregate compared with the flat particle system, but worse than that in the pure round particle system. The agglomerates are of small size and contain either flat and round particles or only round particles. Flat particles tend to agglomerate through the A−A or A−B interactions,

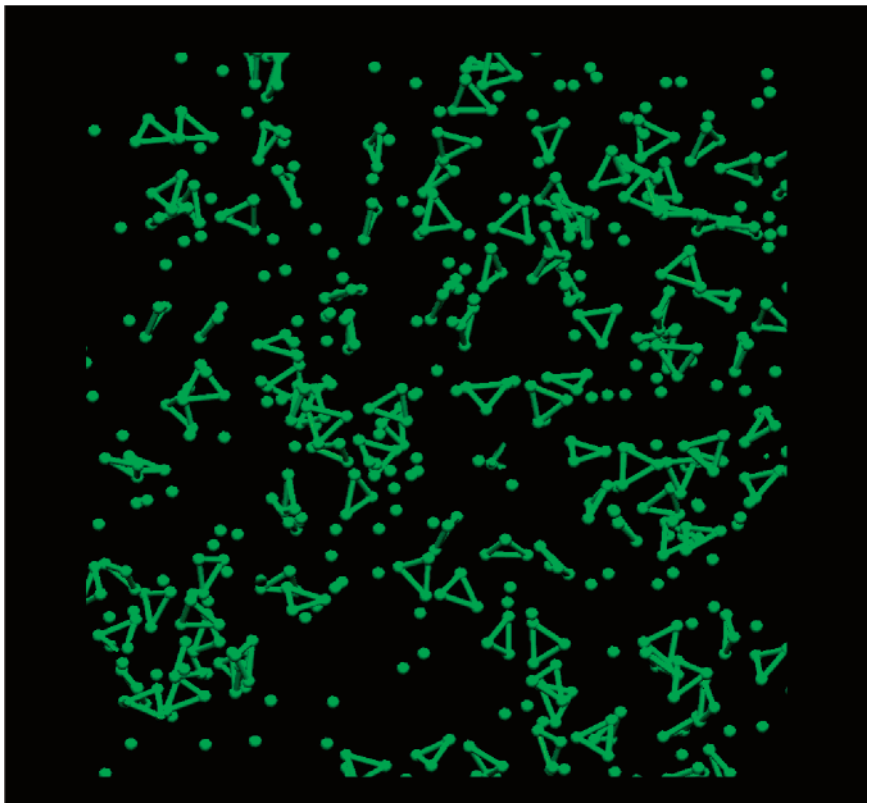

***Figure 9.*** Snapshot from the CG MD simulation for a system of 5000 round and 5000 flat nanoparticles at 1100 K (one-site representation for the round particles and three-site representation for the flat particles).

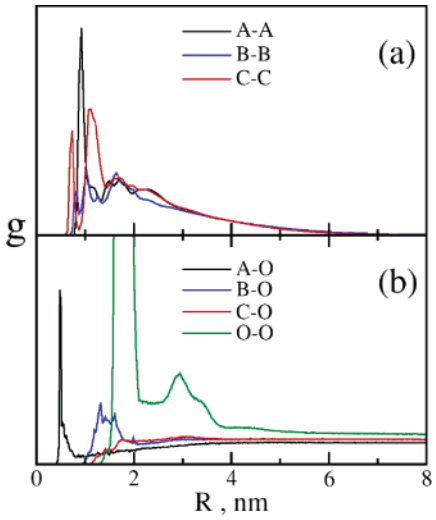


***Figure 10.*** RDFs of the MS−CG MD simulations for ensemble 1—round particles (a) and for ensemble 3—round and flat particles (b). In the upper panel round particles have a three-site representation, A, B, and C and in the lower panel round particles have a one-site representation, O; flat nanoparticles have a three-site representation, A, B, and C.

which are the strongest. The round particles agglomerate primarily among each other and then to the A and B sites of the flat particles. Figure 10 shows the RDFs of the round system (a) reported in Figure 8a and the RDFs for the round/flat system (b) reported in Figure 9. From the width of the peaks, it is possible to derive information regarding the cluster sizes formed during the simulations. For the 10 000-round-particles system, the average cluster size is around 16 nm, and for the round/flat system, clusters of 6 nm are identified between the sites A, B, and C−O.

## Conclusions

The recently developed MS−CG method for obtaining effective pairwise CG force fields from atomistic force and trajectory data has been shown here to be very successful in developing CG models for systems of nanoparticles. The methodology presented is quite general, and in this paper, we applied it to an important real world example, that is, particle formation from combustion sources.

This approach provides a connection between the various time and length scales in the nanoparticles self-assembly problem, together with an unprecedented opportunity for the understanding of the atomistic interactions underlying nanoparticles aggregation and self-assembly. The MS−CG methodology indeed provides an ideal multiscale route for bridging the explicit atomistic representation of the nanoparticles produced by the AMPI simulation method with a more coarse-grained representation necessary to study the agglomeration of the nanoparticles, which in the end can effectively involve millions of carbon atoms.

The agreement in the structural properties is an important result of this methodology because it reveals that even a simple MS−CG model with one or three interaction sites is able to accurately reproduce the structural properties for a system of particles having such a large size and complex geometries. The MS−CG methodology allows rapid parametrization of the CG force fields at the thermodynamic

conditions of interest instead of using "universal" models that increase the reliability of the CG simulations.

Future work will be conducted on mixed systems with a large variety of particles of different sizes and morphologies. Also, the results reported in this paper are relative to the early nucleation of the particles. Once the first nuclei are formed, the process becomes much faster than the one reported in the figures.

**Acknowledgment.** This research is supported in part by a National Science Foundation Nanoscale Interdisciplinary Research Team grant (EEC-0304433).

## References

(1) Homann, K. H.; Wagner, H. G. Chemistry of Carbon Formation in Flames. *Proc. R. Soc. London. Ser. A* **1967**, *307* (1489), 141.

(2) Meyer, H.; Biermann, O.; Faller, R.; Reith, D.; Müller-Plathe, F. Coarse Graining of Nonbonded Interparticle Potentials Using Automatic Simplex Optimization to Fit Structural Properties. *J. Chem. Phys.* **2000**, *113*, 6264.

(3) Shelley, J. C.; Shelley, M. Y.; Reeder, R. C.; Bandyopadhyay, S.; Klein, M. L. A Coarse Grain Model for Phospholipid Simulations. *J. Phys. Chem. B* **2001**, *105* (19), 4464.

(4) Murtola, T.; Falck, E.; Patra, M.; Karttunen, M.; Vattulainena, I. Coarse-Grained Model for Phospholipid/Cholesterol Bilayer. *J. Chem. Phys.* **2004**, *121* (18), 9156.

(5) Marrink, S.; Mark, A. Molecular Dynamics Simulation of the Formation, Structure, and Dynamics of Small Phospholipid Vesicles. *J. Am. Chem. Soc.* **2003**, *125* (49), 15233.

(6) Marrink, S. J.; de Vries, A. H.; Mark, A. E. Coarse Grained Model for Semiquantitative Lipid Simulations. *J. Phys. Chem. B* **2004**, *108* (2), 750.

(7) Brannigan, G.; Brown, F. L. H. Solvent-Free Simulations of Fluid Membrane Bilayers. *J. Chem. Phys.* **2004**, *120* (2), 1059.

(8) Brannigan, G.; Philips, P. F.; Brown, F. L. H. Flexible Lipid Bilayers in Implicit Solvent. *Phys. Rev. E* **2005**, *72* (1), 011915.

(9) Izvekov, S.; Voth, G. A. A Multiscale Coarse-Graining Method for Biomolecular Systems. *J. Phys. Chem. B* **2005**, *109* (7), 2469.

(10) Izvekov, S.; Voth, G. A. Multiscale Coarse Graining of Liquid-State Systems. *J. Chem. Phys.* **2005**, *123* (13), 134105.

(11) Izvekov, S.; Violi, A.; Voth, G. A. Systematic Coarse-Graining of Nanoparticle Interactions in Molecular Dynamics Simulation. *J. Phys. Chem. B* **2005**, *109* (36), 17019.

(12) Izvekov, S.; Parrinello, M.; Burnham, C. J.; Voth, G. A. Effective Force Fields for Condensed Phase Systems from ab Initio Molecular Dynamics Simulation: A New Method for Force-Matching. *J. Chem. Phys.* **2004**, *120* (23), 10896.

(13) Hone, T. D.; Izvekov, S.; Voth, G. A. Fast Centroid Molecular Dynamics: A Force-Matching Approach for the Predetermination of the Effective Centroid Forces. *J. Chem. Phys.* **2005**, *122* (5), 54105.

(14) Izvekov, S.; Voth, G. A. Effective Force Field for Liquid Hydrogen Fluoride from ab Initio Molecular Dynamics Simulation Using the Force-Matching Method. *J. Phys. Chem. B* **2005**, *109* (14), 6573.

(15) Ercolessi, F.; Adams, J. B. Interatomic Potentials from 1st-Principles Calcualtions—The Force-Matching Method. *Europhys. Lett.* **1994**, *26* (8), 583.

(16) Lawson, C. L.; Hanson, R. J. *Solving Least Squares Problems*; Prentice-Hall: Englewood Cliffs, New Jersey, 1974.

(17) De Boor, C. *Practical Guide to Splines*; Springer-Verlag: New York, 1978.

(18) Violi, A.; Izvekov, S.; Voth, G. A. Nanoparticle Agglomeration. *Preprints of Symposia − American Chemical Society, Division of Fuel Chemistry* **2005**, *50* (1), 54.

(19) Violi, A. Modeling of Soot Particle Inception in Aromatic and Aliphatic Premixed Flames. *Combust. Flame* **2004**, *139*, 279.

(20) Violi, A.; Voth, G. A.; Sarofim, A. F. The Relative Roles of Acetylene and Aromatic Precursors during Soot Particle Inception. *Proc. Combust. Inst.* **2005**, *30*, 1343.

(21) Violi, A.; Sarofim, A. F.; Voth, G. A. Kinetic Monte Carlo Molecular Dynamics Approach To Model Soot Inception. *Combust. Sci. Technol.* **2004**, *176* (5−6), 991.

(22) Goel, A.; Hebgen, P.; Vander Sande, J. B.; Howard, J. B. Combustion Synthesis of Fullerenes and Fullerenic Nanostructures. *Carbon* **2002**, *40* (2), 177.

(23) Goel, A.; Howard, J. B.; Vander Sande, J. B. Size Analysis of Single Fullerene Molecules by Electron Microscopy. *Carbon* **2004**, *42*, 1907.

(24) Vander Wal, R. L.; Tomasek, A. J.; Street, K.; Hull, D. R.; Thompson, W. K. Carbon Nanostructure Examined by Lattice Fringe Analysis of High-Resolution Transmission Electron Microscopy Images. *Appl. Spectrosc.* **2004**, *58* (2), 230.

(25) Brooks, B. R.; Bruccoleri, R. E.; Olafson, B. D.; States, D. J.; Swaminathan, S.; Karplus, M. CHARMM—A Program for Macromolecular Energy, Minimization, and Dynamics Calculations. *J. Comput. Chem.* **1983**, *4* (2), 187.

(26) Narsimhan, G.; Ruckenstein, E. The Brownian Coagulation of Aerosols over the Entire Range of Knudsen Numbers—Connection between the Sticking Probability and the Interaction Forces. *J. Colloid Interface Sci.* **1985**, *104* (2), 344.

(27) Smith, W.; Forester, T. R. DL_POLY_2.0: A General-Purpose Parallel Molecular Dynamics Simulation Package. *J. Mol. Graphics* **1996**, *14*, 136.

(28) D'Alessio, A.; D'Anna, A.; Minutolo, P.; Sgro, L. A.; Violi, A. On the Relevance of Surface Growth in Soot Formation in Premixed Flames. *Proc. Combust. Inst.* **2000**, *28* (2), 2547.

CT060030D